ChemistrySelect

Research Article
doi.org/10.1002/slct.202302968

Chemistry Europe
European Chemical Societies Publishing

www.chemistryselect.org

Lysine-Based Two-Component Organogelator: Naproxen Carrier Soft Material

Mehmet Çolak,*[a] Gülşen Kaya,[b] Ali Adnan Hayaloğlu,[b] Nadir Demirel,[c] and Halil Hoşgören[a]

We demonstrated that N^{ε} -alkanoyl-L-lysine ethyl ester/N-alkanoyl-L-phenylalaninate gelling agents were constructed as a two-component gelling strategy and applied as drug carriers in friendly solvents commonly used. Our designs are expected to have an edge in contrast to the other lipid-based systems due to cheap raw materials, reducing the required amount of carrier, low molecular weight, ease of loading, simple dose adjustability, skin spreadability, and improved drug retention times. It could be loaded with Naproxen (Npx) with a high loading efficiency (up to 100% as a percentage of gelator) without gel disruption. A complementary in vitro drug release study under specific pH was conducted and performed at different drug and gelator concentrations. These results reveal that the release of Npx from the supramolecular organogels was significantly retarded with increasing organogelator engagement from 0.46% to 0.92%, the initial release rate considerably reduced, from 18.75% to 7.21%, respectively; that is release rate shows a 2.6-fold decrease; this result showed that the gelator concentration could control drug release. whereas the increasing Npx concentration enhanced it. Altogether, this work produces valuable outcomes, which may be relevant to the pharmaceutical industry, suggesting that new platforms may deliver **NSAID** (non-steroidal anti-inflammotory drug) molecules.

Introduction

A large and growing body of literature has investigated low-molecular-weight gelators (LMWGs) can be modified for different purposes by structure modification and molecular design.[1] Despite well-known polymer gels, various studies have assessed the efficacy of low-molecular-weight gelators (LMWGs) as new soft materials. Supramolecular gels generate this fabric by relying on non-covalent interactions for self-organization into hierarchical. Zeng et al. performed a detailed study on organogels, the relationship between applied solvents and gelators, and their applications in highlighted areas, including exciting potential applications in chemistry, pharmaceuticals, cosmetics, drug delivery, biotechnologies, food technology, tissue engineering, effluent treatment, anti-fouling, anti-icing, and droplet manipulation.[2] However, with the recently increased research in this field, new functional materials have been developed, opening new directions for the application of organogels, such as actuators, supercapacitors, and oil–water separation membranes.[3]

Although relatively few formulations have been investigated for drug delivery despite the vast number of organogels under study. Most organogels are composed of pharmaceutically unacceptable (or untested) gelators and organic solvents. They are being investigated in chemistry or physics departments, where drug delivery may not focus on research.[4] Although the toxicity of selected organic solvents hampers organogels as drug delivery systems, it has some advantages as drug delivery system. Recently, various biomedical and pharmaceutical applications have been improved by synthesizing biocompatible organogels.[5] In particular, for poorly water-soluble drugs comprising ca. 40% of newly discovered chemical entities, oral administration in common dosage forms is problematic.[6] In this perspective, drug carriers have drawn gradually increasing importance and had an enormous impact on interdisciplinary studies, as summarized in reviews on relevant areas.[7,8] Control of drug dose according to amount, place, and time is the main target for drug administration science. While improved control minimizes side effects, it maximizes the therapeutic effect.[9] In addition, excipients should be selected out of biocompatible materials, and using them at minimum levels is requested for other properties.[10] Often, we need to deliver a certain amount of drugs over a long period and clinically useful drug delivery systems that are therapeutically effective. Micro-scale drug delivery systems produced using nanotechnology are used to meet such requirements.[11]

In case the gel formulations as a dermal and topical drug delivery vehicle are expected to include the following desired properties: to use gelator and other ingredients, i.e., all the excipients other than the drug, at a minimum level; to have permeation enhancer property, i.e., to be suitable for cutaneous dermal and topical drug administration; to contain ingredients such as gelator and gelation medium that are made of biocompatible materials and to include functional groups recognized by our body. Gel and gelation medium also requires a longer shelf life as in bioactive materials and cosmetic applications.[12] In addition, the drug carrier should not be toxic,

[a] *Dr. M. Çolak, Prof. H. Hoşgören*
Department of Chemistry, Faculty of Science & Art, University of Dicle, 21280, Diyarbakir, Turkey
E-mail: mcolak@dicle.edu.tr

[b] *Dr. G. Kaya, Prof. A. Adnan Hayaloğlu*
Department of Food Engineering, İnönü University, 44280, Malatya, Turkey

[c] *Prof. N. Demirel*
Department of Chemistry, Faculty of Science & Art, Kırşehir Ahi Evran University, 40100, Kırşehir, Turkey

irritating, or skin-sensitizing in topical and transdermal applications. By retaining the desired properties while overcoming undesirable properties, therapeutic efficacy can be improved.[13] These activities can be achieved using physical, chemical, and biological ways. The viscoelastic gel is an important alternative among different drug carrier platforms used to formulate active drug substances to protect its payload from enzymes or low stomach pH.[14]

Most of the non-steroidal anti-inflammatory drugs used today have restrictions due to gastric intolerance. Various approaches have been suggested to adopt the parent non-steroidal anti-inflammatory drug molecule to reduce gastric toxicity.[15] Besides its essential pharmacological activities, Naproxen has severe side effects due to its acidic functional group. Due to gastrointestinal problems (ulcers) during oral administration of NSAID (non-steroidal anti-inflammatory drugs), cutaneous administration of these drugs for relief of joint pain and inflammation will provide many advantages. On the other hand, using the skin as a route for Npx delivery attracts much attention. It is seen as a potential route for skin and systemic drug administration due to its easy accessibility. As a result, research into transdermal drug delivery has become widespread in the last two decades.[16] The gelator structure is constructed using a biomolecular precursor to enhance its biocompatibility and biodegradability potentials. As a strategy in this context, one of the components of the gelator includes a biological molecule/precursor to improve its biocompatibility and biodegradability.[17] In cutaneous NSAIDs administrations, the formulations commercially available in gel form are polymeric hydrogels. However, polymeric hydrogels cannot meet the 'minimum excipient' condition necessary for used excipients due to polymeric structure. In addition, the use of a protective ingredient (excipient) is required due to the contamination problem in hydrogels, which causes some negative situations, such as the administration of many components. The use of low-molecular-weight organogelators (LMWOG's) instead of polymeric gelators does not cause contamination problems. We previously reported the synthesis and gelation capabilities of N$^{\varepsilon}$-alkanoyl-L-lysine ethyl ester/N-alkanoyl-L-phenylalaninate gelling agents in pharmaceutical fluids.[18] These original gelators will be assessed for the first time as carriers in this study for the non-steroidal naproxen drug. Consequently, five artificial gelling agents formulated as $\mathbf{B_mA_n}$ types, including [N^{ε}-palmitoyl-*L*-lysine ethyl ester/*N*-lauroyl-*L*-phenylalaninate($\mathbf{B_1A_3}$), N^{ε}-palmitoyl-*L*-lysine ethyl ester/*N*-myristoyl-*L*-phenylalaninate ($\mathbf{B_1A_4}$), N^{ε}-palmitoyl-*L*-lysine ethyl ester/*N*-palmitoyl-*L*-phenylalaninate ($\mathbf{B_1A_5}$), N^{ε}-myristoyl-*L*-lysine ethyl ester/*N*-lauroyl-*L*-phenylalaninate($\mathbf{B_2A_3}$), N^{ε}-myristoyl-*L*-lysine ethyl ester/*N*-palmitoyl-*L*-phenylalaninate ($\mathbf{B_2A_5}$)] were employed in pharmaceutical fluids for the drug carrier soft materials as a two-component gelators strategy. In this study, Naproxen was chosen as a model drug because it is a potent non-steroidal anti-inflammatory drug used in the acute and long-term treatment of rheumatoid and osteoarthritis.

In the last 15 years, many studies have examined the relationship between rheology and release profiles and the effect of rheological properties on drug release rates from gels. Rheology and other experimental techniques (NMR relaxation measurements) used to characterize organogels are excellent methods for predicting the behavior of semi-solid systems and characterizing the structural strength during topical use.[19] To accomplish this goal, we selected five structurally diverse (differing in the length of hydrocarbon chain bearing on the acidic and basic components) small molecule gelling agent (SMGA).

Materials and method

All chemicals were purchased from commercial sources (Merck, Fluka, and Sigma-Aldrich) and used without any further purification if not mentioned otherwise. Myristic acid isopropyl ester (**MIE**), and palmitic acid ethyl ester (**PEE**), were prepared by protocols described in the literature. The desired fatty acid isopropyl esters were obtained in high yields (88–94 %) by treating the appropriate fatty acid with an alcohol in significant molar excess in the presence of a catalytic amount of dehydrated p-toluene sulfonic acid.[20]

Apparatus for measurements

UV-Vis measurements were carried out using VARIAN UV1010M211 CARY 100 BIO UV-visible spectrophotometer. Rheological measurements were carried out with an Anton PAR MCR 301 stress rheometer with a 20 mm cone plate and 0.047 mm the width of the gap. pH measurements were carried out with a METTLER TOLEDO GmbH 8603 pH meter, calibrated with standard buffers. Fourier transform infrared spectroscopy (FTIR) using Mattson 1000, ATI UNICAM machine was employed to furnish information about the functional groups present in the prepared formulation.

Gelators synthesis

Formulated as $\mathbf{B_mA_n}$ types [N^{ε}-palmitoyl-*L*-lysine ethyl ester/*N*-lauroyl-*L*-phenylalaninate ($\mathbf{B_1A_3}$), N^{ε}-palmitoyl-*L*-lysine ethyl ester/*N*-myristoyl-*L*-phenylalaninate ($\mathbf{B_1A_4}$), N^{ε}-palmitoyl-*L*-lysine ethyl ester/*N*-palmitoyl-*L*-phenylalaninate ($\mathbf{B_1A_5}$), N^{ε}-myristoyl-*L*-lysine ethyl ester/*N*-lauroyl-*L*-phenylalaninate ($\mathbf{B_2A_3}$), N^{ε}-myristoyl-*L*-lysine ethyl ester/*N*-palmitoyl-*L*-phenylalaninate ($\mathbf{B_2A_5}$)] two-component gelators systems are shown in Scheme 1. The two-component gelator systems were synthesized according to the literature procedure.[18]

Drug Loading and Release

Considering MGC and rheological data about $\mathbf{B_mA_n}$ -type gelators, ($\mathbf{B_1A_3}$) and ($\mathbf{B_2A_3}$) gelators were found applicable and convenient in the drug release studies. The loading of Npx into the gel network was carried out using the procedure described in the literature.

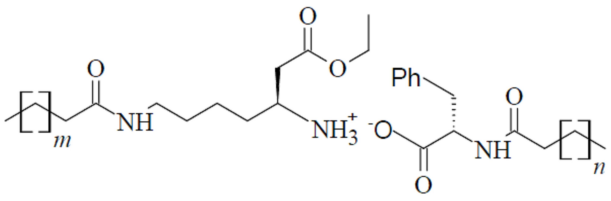

B_1A_3 m = 13 ; n = 9 B_1A_4 m = 13 ; n = 11 B_2A_5 m = 11 ; n = 13

B_2A_3 m = 11 ; n = 9 B_1A_5 m = 13 ; n = 13

Scheme 1. Two-Component Gelators Structures.

Determination of drug loading capacity

Gelator concentrations were kept to a minimum (1 mg above MGC). The gelator and drug were dissolved in 1 mL of organic fluids at hot, and the mixture was allowed to cool. Each time, the amount of the drug was increased by 1 mg. The process continued until the structure of the gel network collapsed. The amount of drug at the collapse point of the gel is defined as the maximum drug loading capacity. The drug loading is made slowly, and the dissolution of the drug is provided by heating a gel matrix in each case. The gel structure is controlled whether it is collapsed by cooling at room temperature. The maximum drug loading capacity represents the total amount of drug at the point where the gel structure collapsed. The gelator's drug loading capacity, which is at the **MGC** in different solvents (1 mL), was obtained by slow successive addition of Npx to the prepared gels until the gel structures are reproduced. The gelator's maximum drug loading capacity (**MDLC**) was found from the following equation (Eq. 1)

$$MDLC = \% \ w_d/w_g x100 \quad \text{(Eq. 1).}$$

where w_d is the weight of the drug loaded in the gel and w_g is the weight of the gelator in the gel matrix.

Rheological studies

Phenylalanine attachment in the acidic components of **B_1A_3**, **B_1A_4**, **B_1A_5**, **B_2A_3**, **B_2A_5** gelators was chosen as a gelling agent for the carrier matrix. The rheology of various gels was investigated concerning the structure of gelators and gelling fluid. The effect of gelator structure on the viscoelastic properties of gels was evaluated for the **B_1A_3**, **B_1A_4**, **B_1A_5**, **B_2A_3**, **B_2A_5** gelators in liquid paraffin (LP). Besides **B_1A_3**, **B_2A_3** gelators were also examined in different fluids **(MIE, PEE, LP)** based on the fluids' nature. The experiment was done in frequency sweep as well as strain sweep mode. The frequency scanning was performed at a constant strain of 0.1 %, while strain scanning was performed at a constant frequency (10 rads^{-1}). Before measuring the linear viscoelastic region (LVR) was determined by measuring the storage or elastic modulus and loss or viscous modulus as a function of the strain constant angular frequency (10 rads^{-1}). Storage modulus (G′), loss modulus (G′′), and loss angle (δ) values were used in the oscillation measurements made for the characterization of the samples. The G′ reveals the system's ability to store elastic energy associated with recoverable elastic deformation and is an indicator of elastic behaviour. The *G′′* measures the dynamic viscous behaviour related to energy dissipation associated with unrecoverable viscous loss. The relationship between *G′*, *G′′*and tan δ is Eq.2.

$$\tan \delta = G''/G' \quad \text{(Eq. 2).}$$

The LVR and the viscoelastic properties of the **B_mA_n** gels with Npx loaded and unloaded the dynamic oscillation stress sweep test determines forms. In the oscillation stress sweep test, the gel was subjected to constantly increasing stress. The stress was increased until the structure of the gel deteriorated. The frequency was kept at a constant angular frequency (10 rads^{-1}) throughout the test. These tests allowed the determination of the LVR, which corresponds to strain amplitude-independent properties and the determination of the viscoelastic modulus up to frequency only. In addition to determining the endpoint of the LVR, the substance G′ dropped 10 % from the linear level under dynamic oscillation tests. The stress at the crossing-over point when the G" value was equal to G′, and the significance of tan δ was 1.[21,22] Frequency scanning was performed with constant strain in the range of 0.1–10.0 Hz at 25°C after determining the LVR. The oscillation stress for frequency sweep measurements was chosen as 1.3 Pa based on the strain sweep results to confine the samples within the linear viscoelastic region. A dynamic oscillation frequency sweep test was used to determine the gels′ capability to resist structural changes under the increased frequency. The complex viscosity η^* was determined under the same conditions, and it was determined that the gel was in the elastic linear region by frequency scanning test. The results show the properties of an intact gel. In addition, the slope values of the curves were calculated to investigate the frequency dependence of the samples.[23] Rheological analysis was performed for all formulations considering free and loaded Npx compositions for the determination of elastic (G′) and viscous (G′′) modulus and viscosity (η*). All results for other organogel formulations are presented in Table 1. Before strain and frequency sweep measurement, prepared gels were allowed to be set for 2–

Table 1. The oscillation stress sweep test results for the Naproxen loaded and unloaded B_mA_n gelators in different fluids at 25 °C. n = 6; at 0.0681 % strain.

Gelator/Fluid	*tanδ = G″/G′*	Storage Modulus[a]	Crossing over point	End point LVR	Loading capacity[b]	η*[Pa·s]	*G′/G″* ratio[d]
	L/U[c]	G′(Pa)L/U	(Pa)L/U	(Pa)L/U	L/U		Loaded form
B2 A3/LP	0.225/0.205	5888/3288	76/65	13.39/33.9	35(0.17)[c]	0.6/19	5888/1720 = 3.42
B2 A3/MIE	0.525/0.15	8912/5358	6/30.15	2.14/5.43	83(0.29)[c]	348/1050	8912/4330 = 2.05
B2 A3/PEE	**0.093/0.21**	**38300/1367**	**267/6.9**	**123.02/2.05**	25(0.12)[c]	**7.0/753**	**39300:4530 = 8.72**
B1 A3/LP	**0.20/0.16**	**23908/1659**	**115/71**	**15.99/24.5**	50(0.17)[c]	358/525	**23908/1200 = 19.1**
B1 A3/MIE	**0.123/0.16**	**7943/5248**	**92.7/6.5**	**17.37/5.43**	**100(0.35)[c]**	**125/97**	**7943:1400 = 5.67**
B1 A3/PEE	0.177/0.147	7320/11194	13.7/25	5.05/11.48	50(0,23)[c]	139/202	7320:1300 = 5.63

[a] G′ at the end value of LVR (w/w %); [b] $w_{drug}/w_{gelator}\times100$; [c] ^{w}drug/^{w}gel×100; L/U: Loaded/unloaded; in all the loading test, gelator concentration was taken: 7 mgmL^{-1}; Npx; 1 mgmL^{-1}. η*:complex viscosity (from frequency sweep test); [d] G′/G″ ratio at the end value of LVR.

3 hours. Then, the gelator concentrations higher than **MGC** (7 mgmL^{-1}) in different fluids (**LP**, **MIE**, and **PEE**) as Npx-free and loaded forms were applied to explore rheological measurements. In addition, the oscillatory measurement test was performed with different concentrations of Npx and gelator in (**B_1A_3**)/**MIE** and (**B_2A_3**)/**MIE** gel systems, respectively. Likewise, to evaluate the stability of the formulation, the frequency sweep test was made with **B_1A_3**/**MIE** gel system, measuring the same sample immediately and after preparation for 50 days. Oscillatory measurements were used to evaluate the stability of the formulation immediately after preparation and up to 50 days to obtain G′, G″, and η* for each formulation. All tests were repeated at least three times for each batch, and all measurements were made from individual samples.

Fourier transform infrared spectroscopy

Fourier transform infrared spectroscopy (FTIR) was employed to furnish information about the functional groups present in the prepared formulation. The FTIR spectra of pure drug (Npx), B2 A3/LP, and B2 A3/LP-Npx formulation were carried out using Mattson 1000, ATI UNICAM machine at 25 °C and wave number ranging from 4000 to 400 cm^{-1}. Whether any drug-excipient interaction was detected in the B2 A3/LP-Npx formulation using the FTIR technique as described in the literature (Sharma 2018). This confirmed the absence of any drug-excipient interaction in the B2 A3/LP-Npx formulation.

Release studies

The two-component gelling system, containing Npx, is prepared as described in the literature method.[24] The Npx-loaded gel was kept in a constant temperature bath at 25 °C for four hours. Then, 6 mL of phosphate buffer of different pH was carefully placed on top of each drug-loaded gel matrix. The release behaviour of Npx was investigated for various gelling liquids and different pH values, depending on the gelator and drug concentration. Release tests were carried out under static conditions. Npx stock solutions(160 mg L^{-1}) were gradually diluted to obtain a calibration curve, and maximum absorbance was measured at 262 nm using a UV-Vis spectrometer. The calibration curves showed perfect linear relationships in the range of 0–20 mg L^{-1} Npx concentration and maximum absorbance. At the designed intervals, 3 mL of the supernatant solution was removed and filtered using filter paper. After, 3 mL of buffer solution was added to the Npx-loaded gel matrix in the test tube. The absorption spectrum of each solution was recorded at the previously determined λmax of the active drug agent. The concentration of the Npx released from the organogel was estimated based on the calibration curves. All the tests were done at least in triplicate.

Solvent effect on the drug release

The solvent effect was carried out with (**B_1A_3**) and (**B_2A_3**) gelators in **MIE**, **PEE**, and LP due to their high drug loading capacity and having the lowest **MGC** in these fluids. It is seen that from the cumulative release % vs. time (t) graph, drug release could be controlled with different gelling fluids. Therefore, the release rate of Npx (1.5 mg) depending on the fluids was performed **B_1A_3** (5 mg) and **B_2A_3** (4 mg) gelators in three different solvents (1 mL of MIE, PEE, and LP) at pH 7.4 and 25 °C.

The effect of pH on the release of Npx

The effect of pH on the release rate of Npx (1.5 mg) was studied with a **B_1A_3** (5 mg) gelator prepared in **MIE** due to the high Npx release rate in this fluid at three different pH (7.4, 7.0, 5.5) at 25 °C.

Effect of Drug Concentration

Drug concentration was explored with the (**B_1A_3**)/**MIE** gel system by considering drug loading capacity and solvent effect on the cumulative release %. Experiments were made with **B_1A_3**

(5 mg) gelator in MIE (1 mL) at 25°C and pH 7.4 at different Npx concentrations.

Effect of Gelator Concentration on the Drug Release

Gelator concentrations affected the cumulative release rate since good gelation ability, and high loading capacity (**B_1A_3**)/**MIE** and (**B_2A_3**)/**MIE** systems were exploited. Therefore, the drug release study was performed with Npx (1.5 mg) loaded gel at 25 °C and pH 7.4 with different concentrations (4, 5, 8 mg) of (**B_2A_3**) and (**B_1A_3**) gelators in **MIE**.

Drug loading into the gel matrix

Preorganogel networks have several advantages compared with conventional sorbents, such as clays, zeolites, silica, activated carbon, and natural fibers. First, the mass uptake for gel sorbents is practically higher (up to 99 wt.%). Other advantages include the potential for reversible and selective sorption.[26]

Taking into consideration of gelation abilities and **MGC**, (**B_1A_3**), (**B_2A_3**), (**B_1A_4**) and (**B_2A_5**), (**B_1A_5**) gelators[18] having phenylalanine part in their structures of the acidic component was tested as a drug carrier matrix. All the gelators having phenylalanine, a.a. in the acidic components, gave good gels in LP; therefore, Npx loading capacities were tested in this fluid. The Npx loading experiments were also performed in **MIE** and **PEE** fluids with (**B_1A_3**) and (**B_2A_3**) gelators because of their high loading capacities and low **MGC** in these fluids. Comparison images of unloaded and loaded gel forms were shown in Figure 1. The loading capacity is moderately dependent on the fluid polarity and lipophilicity of the gelator. The loading capacity of (**B_1A_3**), (**B_1A_4**), (**B_1A_5**), **and** (**B_2A_3**), (**B_2A_5**) gelators (having the same amino acid, phenylalanine, in the part of acidic component) in LP were found **50%**, **66%**, **86%**, **and 35%**, **75%** (as a drug/gelator, w/w %), respectively (Table 2). These results show that the different fatty acid chains in the acidic and basic components impact the loading capacity of gels. As shown in (Table 2), drug loading capacity in **LP** increased with the increasing fatty acid esters (**FAE**) chain length on the acidic and basic components. Maximum loading capacity (DLC_{max}) was obtained with (**B_1A_3**)/**MIE** among all the tested fluids. For this reason, the (**B_1A_3**)/**MIE** system was chosen as a drug carrier; and tested for the Npx release experiment. In topical and transdermal drug delivery, FAE and related alcohols as enhancers for drug permeability are of great interest. Since drug loading capacity was evaluated depending on the **FAE**'s nature, the entrapment of small drug molecules within an **LMWG** gel matrix could be loaded in quite a simple way. Figure 1 For example, with (**B_1A_3**)/**MIE**, as the carrier for Npx, 100% (drug/gelator, w/w %) loading could be achieved without gel disruption.

Release kinetics of organogel formulation

The release of gels prepared with different Npx concentrations in 1 mL MIE and 5 mg gelator was examined at pH 7.4 and 25 °C. The experimental data obtained are given in Table 3. In

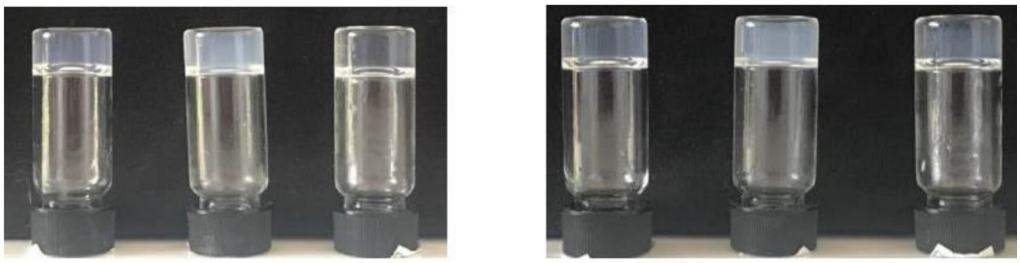

Figure 1. Comparison images of unloaded gels (left) and Npx loaded gels (1.0 mg) (right) composed of B_1A_3/LP, B_1A_3/MIE and B_1A_5/LP, respectively. All the gels were prepared with (7.0 $mgmL^{-1}$) gelators in 1 mL of fluids.

Table 2. The ratio of the viscous and elastic moduli ($tan\delta = G''/G'$); endpoint of LVR and crossing over point ($G' = G''$) values and loading capacity of B_mA_n/LP gel samples as a function of oscillation stress measurement.

TCN[a]	G′/G″ ratio	tanδ = G″/G′	Loading capacity[b]	η*[Pa·s][d]	Crossing over point	End point LVR	Storage Modulus[c]
	Loaded form	L/U		L/U[e]	(Pa)L/U	(Pa)L/U	G′(Pa)L/U
B1 A3/28	**22908/1200 = 19.1**	**0.158/0.204**	50(0.17)c	358/525	**115/70**	**15.99/24.5**	**22908/1659**
B1 A4/30	323.6/72.4 = 4.47	0.189/0.187	66(0.23)c	16/34	7.54/0.98	2.27/0.316	323.6/95.5
B1 A5/32	107.2/24.1 = 4.45	0.219/0.11	86(0.30)c	215/148	1.29/6.2	0.162/1.29	107.2/525
B2 A3/26	**5888/1720 = 3.42**	**0.225/0.205**	35(0.17)c	**30.6/19.5**	**76/65.1**	**13.39/33.9**	**5888/3288**
B2 A5/30	**8912/1550 = 5.74**	**0.125/0.176**	75(0.34)c	**25/69**	**98.2/4.4**	**29.17/1.3**	**8912/575**

[a] TCN: Total carbon number of gelator; [b] (w/w %): $w_{drug}/w_{gelator}\times100$; [c] $W_{drug}/W_{gel}\times100$; [d] G′ at the end value of LVR; in all the loading test: gelator concentration was taken: 7 $mgmL^{-1}$. L/U: Loaded/unloaded; [e] η*:complex viscosity.

Table 3. Model Fit Correlation Coefficient (R^2) for the B_1A_3/Npx gel system at first 10 h.

	Model Fit Correlation Coefficient (R^2)					
Npx (mg)	Higuchi Model	Hixson Crowell Model	Peppas Model	zero order model	Firsth Order model	The most compatible model
1.5	**0.9891**	0.9462	0.9522	0.9661	0.9468	Higuchi Model
3	**0.9818**	0.9355	0.9468	0.9553	0.9596	Higuchi Model

[Not] B_1A_3/Npx gels in MIE at 25 °C. pH 7.4 at different drug concentrations.

addition, the kinetics of drug release from the organogel system is determined by the Ritger-Peppas model. The equation 3 was expressed as follows:

$$Mt / M\infty = \mathbf{k}^{n} \quad \text{(Eq. 3).}$$

Mt is the absolute cumulative amount of drug released at time t, M∞ is the absolute cumulative amount of drug released at infinite time, k is a constant reflecting the design variables of the system, and n represents the diffusion index, which could be used to characterize the mechanism of release. When $n \leq 0.43$, it reflects the release behavior is dominated by diffusion. While if $n \geq 0.89$, the release mechanism of drug is erosion. When the value is between 0.43 and 0.89, it means the release mechanism is controlled by a combined action of both diffusion and erosion.[25]

Results and discussion

Chemistry

All our synthesized lysine-based two-component systems form the salt formation of acidic and basic components. Each one contains the two-amide linkage, which gives the best gelating property of all five compounds confirmed by previous research. The hydrophobic long fatty acid alkyl chains and their salt formation of acidic and basic component structures and the two-amide linkage can accelerate hydrogen bonds′ formation. Therefore, hydrogen bonds′ formation may contribute to the gelation process. Besides, both fatty acid groups and amino acid parts are harmless, biodegradable, and biocompatible, suitable for biomedical applications. Here, compounds 1–5 were easily prepared by salt formation of an acidic and basic component having different amino acid parts and different alkyl chains on the structures. Although the chemical structures of these synthesized compounds are similar, they all have different fatty acids in their $\mathcal{E}$-amino groups of *L*-lysine linking and with different amino acids in the acidic component. Among phenyl alanine-bearing, acidic components have the best gelating capability for organic solvents due to the existence of π-stacking besides the hydrogen bonding capability of two amide linkage and weak van der Waals interaction between fatty acid chains linkage on the acidic and basic components.

Rheological measurement

Frequency sweep experiments conducted by applying a constant shear strain within the LVR for each sample confirmed that all gel systems exhibit "solid-like" behaviour. The linear viscoelastic region was determined for each sample through strain sweeps at 10 rad/s. G', G'', and δ for the Npx loaded and its unloaded forms were determined within the LVR.

G' and G'' were found frequency independent, in the range from 0.1 to 10 Hz, with G′ always more significant than G″ (Figure 2) and the loss factor ($tg\delta = G''/G'$) is low at all frequencies. The sample is qualified as gels when $G' > G''$ and 'strong gels' are defined when the relation between G″ and G′ the loss factor ($tg\delta = G''/G' \leq 0.1$),. It is shown that in Fig 3 a and b, G' and G'' is plotted as a function of oscillating frequency, corresponding to the **B_1A_5/LP** and **B_1A_3/PEE** gels Npx free and loaded forms, respectively. G' and G'' do not vary significantly with the range of applied angular frequency (ω) and do not cross each other ($G' > G''$) throughout the experimental region (Figures 3). For all fluids tested, G′ is higher than G′ in the entire frequency range. This result shows that elastic behaviour dominates viscous behaviour. When the G′ and G" curves were represented, their double logarithmic charts, parallel straight lines across the entire frequency range show only a slight slope indicating that elastic behaviour dominates viscous behaviour (Figure 4).

Interestingly, the Npx-loaded B_1A_3 sample showed the highest stiffness among these two-component gelling systems, constructed with B_1 and A_3 components as basic and acidic parts. The G′ and G″ curves indicate the presence of a stable and rigid gel phase material. This figure demonstrates the very high stability of the Npx loaded **B_1A_3** in **LP** (G'/G'' ratio is 19.1) beside of **B_1A_3/LP** and **B_1A_3/MIE**, **B_2A_3/PEE** gave good rheologic data in their Npx loaded forms than its unloaded forms: They have low loss factor ($tg\delta = G''/G'$), lasting LVR: The end value of the LVR determined whether the steady-state structure was disrupted or even destroyed. (Table 1 and Figure 5).

The mechanical resistance of a dermatological product is essential when it is removed from the container, spread on the skin, or applied to the skin. As Table 1 represents, all the Npx-loaded gel systems have a lower viscosity than their unloaded forms, except that **B_1A_3** has a more viscous nature in **MIE** than its unloaded form. The oscillation stress sweep test showed that Npx loaded **B_2A_3/PEE** formulation had the most viscoelastic structure, the storage modulus and crossing over point values

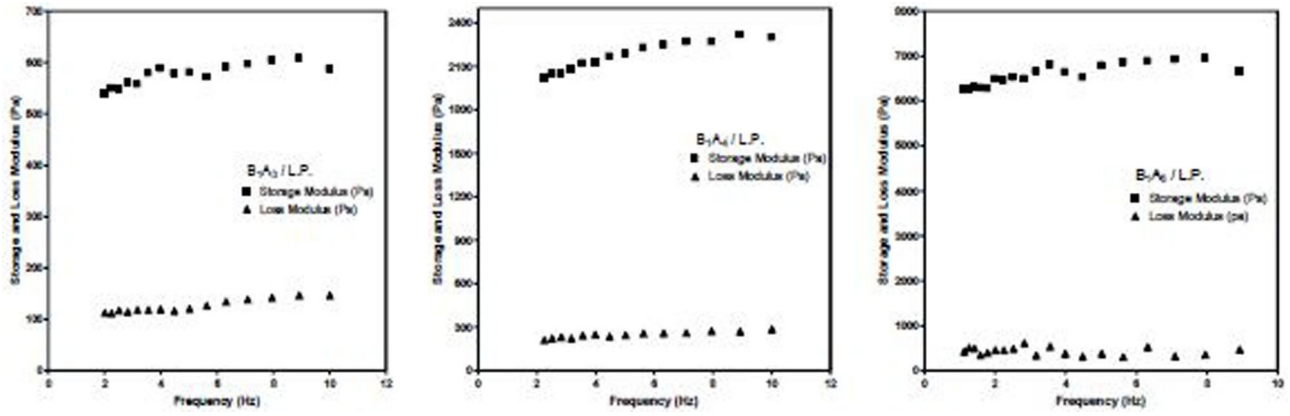

Figure 2. The elastic and viscose modulus is plotted versus oscillating frequency, depending on the different chain lengths of the acidic components: B_1A_3, B_1A_4, and B_1A_5. Gelators in liquid paraffin at 7 mgmL^{-1} at 25 °C. G′, filled square; G″, filled triangle.

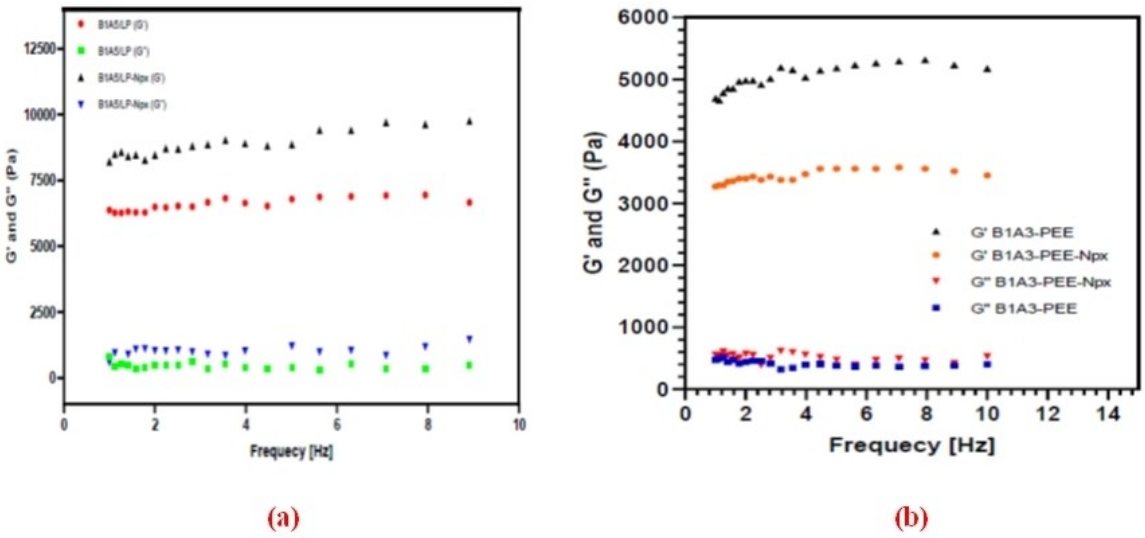

Figure 3. Variations of *G′* and *G″* as a function of frequency for the Npx free and loaded forms of B_1A_5/LP **(a)** and **B1 A3/PEE (b)** gels at 25 °C. G′, blue and green; G″, purple and brown. Gelator concentration: 7 mgmL^{-1}, Npx; 1 mgmL^{-1}. Each curve presents the mean value of three tests.

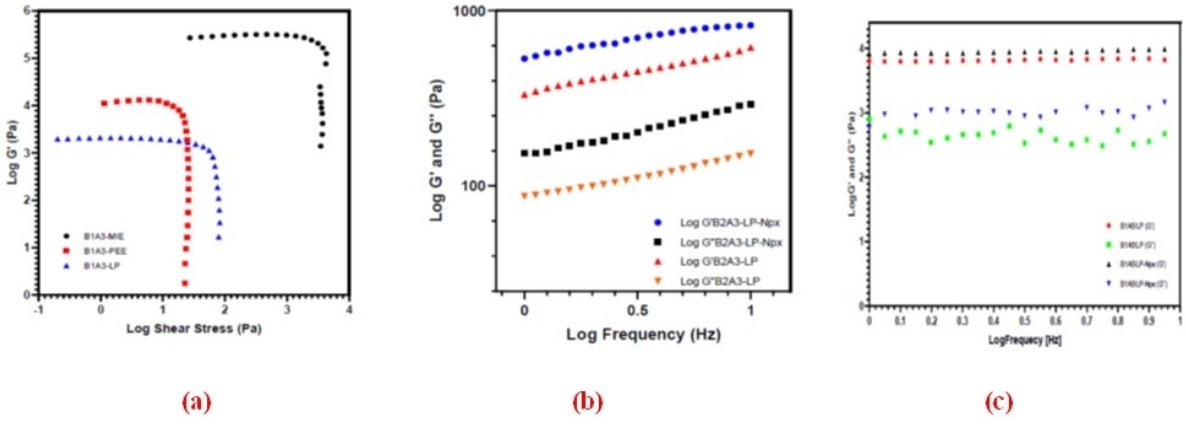

Figure 4. a) Double logarithmic graph Npx loaded and unloaded forms of B_1A_5/LP gels are plotted versus log oscillating frequency measurement at 25 °C, depending on the acidic component chain length. **b)** Double logarithmic graph Npx free and unloaded forms of B_2A_3/LP gels systems. **c)** Log G′ and G″ are plotted for the Npx free and loaded forms of B_2A_5/LP gels samples as a function log oscillating frequency at 25 °C. The log storage and loss modulus is plotted as a function of log oscillating frequency measurement at 25 °C; Gelator concentration: 7 mgmL^{-1}, Npx: 1 mgmL^{-1}. Each curve presents the mean value of three tests.

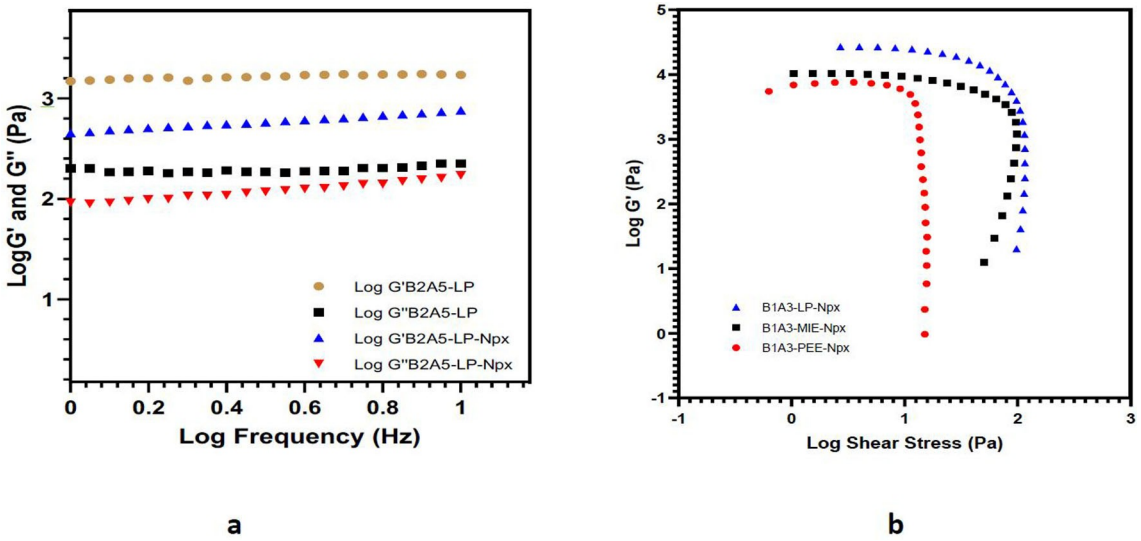

Figure 5. The endpoint of LVR as a function of frequency (a) and shear stress (b) respectively B_1A_3 gel (Npx unloaded) in the different fluids; gelator was taken 7 mgmL^{-1}. Each curve represents the mean value of three tests.

were higher than other B_2A_3 formulations, even **unloaded B_2A_3/LP** has the most extended LVE range Table 1.

The LVR of the **B_2A_3/PEE** formulation was the most comprehensive and differed from other B_2A_3 formulations only in the oil component (Table 1). This difference is because the ethyl palmitate used in **B_2A_3/PEE** formulation has two carbons more in the fatty acid chain than the isopropyl myristate used in **B_2A_3/MIE** formulation. Therefore, the longer hydrocarbon chain of oil made **B_2A_3/PEE** formulation more elastic for the Npx (Tables 1). .The end value of G' at the LVR of Npx loaded **B_1A_3/LP** was 15.99 Pa those of **B_1A_3/MIE** and **B_1A_3/PEE** gel systems were found 17.37 and 5.05 Pa, respectively (Table 1). And similar results were obtained for Npx-loaded **B_2A_3/PEE**, **B_2A_3/LP** and **B_2A_3/MIE** gel systems; were found at 123.02 Pa, 13.39 Pa and 2.13 Pa, respectively (Table 1). Due to the highly intermeshed structure, Npx-loaded **B_2A_3/PEE** has a larger linear region. Therefore, this formulation appears to be more resistant to mechanical stress. Furthermore, in the application, a low yield value means easy spreadability. Therefore, the consistency in this formulation will be perceived as soft and easily spreadable on the skin. Such property is of great importance for a dermal product, mainly when applied to inflamed, sensitive skin Figures 10 and 11. The strain sweep measurement showed that solvent had a noticeable impact on the rheological properties, which might be ascribed to their different aggregations. Moreover, strain sweep measurement revealed that B_2A_3/PEE gel's modulus value was higher than that of the corresponding organogel.

Oscillatory measurement of Npx unloaded and loaded B_2A_3, B_2A_5, and B_1A_3, B_1A_4, B_1A_5 gelators in the liquid paraffin was shown in (Table 2, Figure 7 and 8, respectively) as a function of different components chain length. The structure

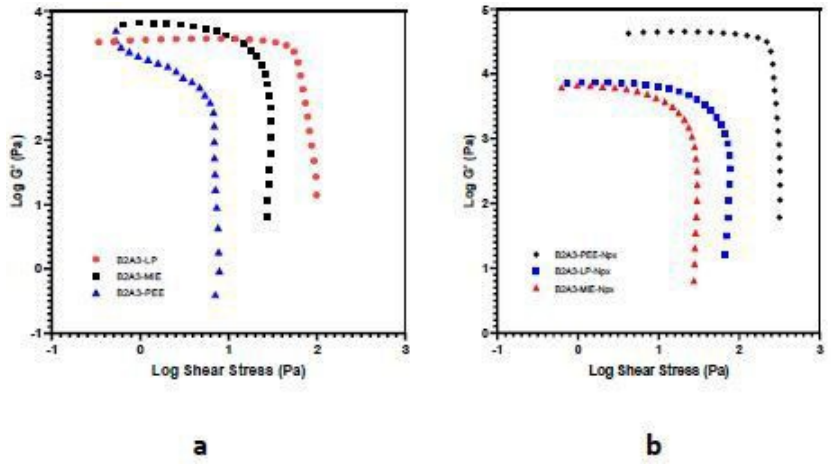

Figure 6. The endpoint of linear viscoelastic range as a function of shear stress: a) B_2A_3 gel (Npx unloaded); b) Npx loaded B_2A_3 gels in the different fluids; gelator was taken 7 mgmL^{-1}. Each curve represents the mean value of three tests.

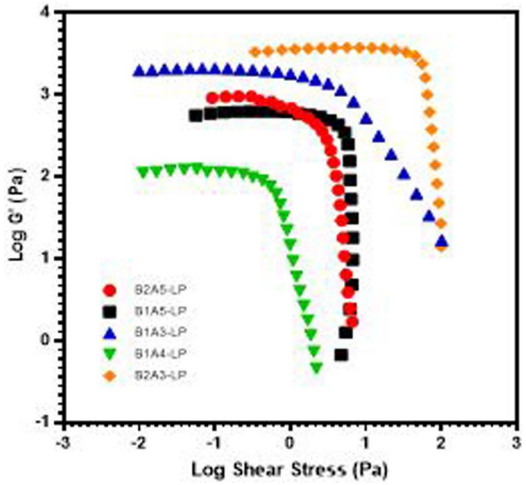

Figure 7. The endpoint of linear viscoelastic range as a function of shear stress: B_mA_n gels (Npx unloaded) in LP; gelator concentration was taken 7 mgmL^{-1}. Each curve presents the mean value of three tests

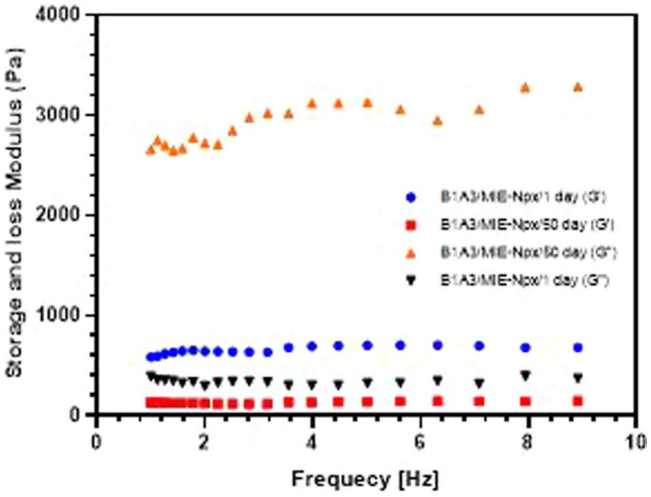

Figure 9. Effect of storage time on the viscous and elastic moduli for the B_1A_3/**MIE** gel samples depending on the oscillating frequency measurement at 25 °C. The time-dependent measurement was made at two different waiting times: 1 day and 50 days after sample preparation. G′, blue and green and G″, gold brown, and purple are shown. Gelator concentration: 7 mgmL^{-1}, Npx: 1 mgmL^{-1}. Each curve presents the mean value of three tests.

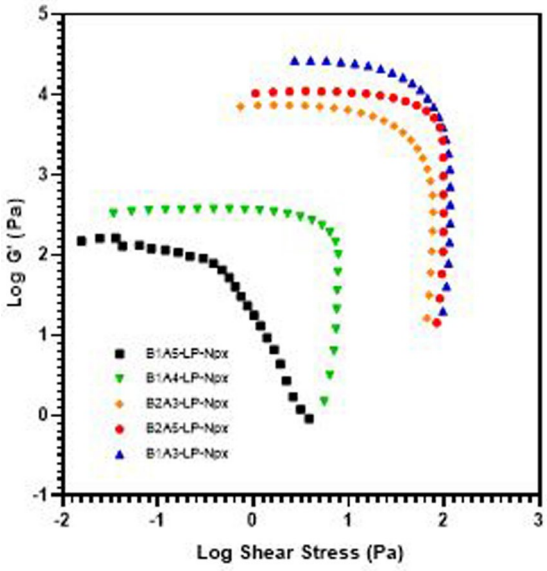

Figure 8. The storage modulus of B_mA_n gelators in the liquid paraffin as a function of shear stress. The gelator concentration was taken at 7 mgmL^{-1}. Npx; (1 mgmL^{-1}). Each curve presents the mean value of three tests.

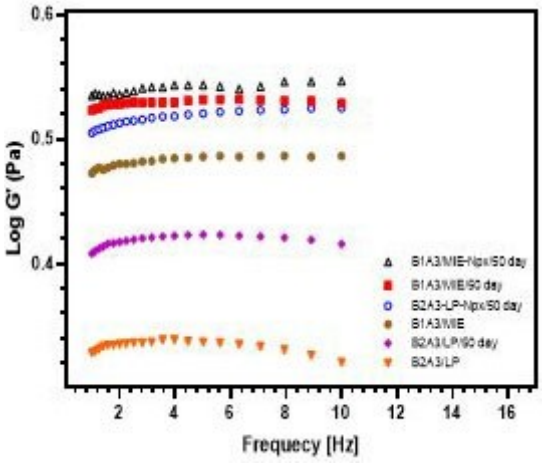

Figure 10. The log G′ of gels is plotted versus oscillating frequency at two different waiting times: in a day and after storage 50 days at 25 °C. Gelator in B_2A_3/**LP** and B_1A_3/**MIE** gels : (7 mgmL^{-1}), Npx: (1 mgmL^{-}1). Each curve presents the mean value of three tests.

of B_1A_5/**LP** and B_1A_4/**LP** systems were broken down at small stress values when others showed no changes by applying moderate strain. We can explain the short linear region of B_1A_5/**LP** and B_1A_4/**LP** matrix systems due to inappropriate lipophilic/hydrophilic balance produced from long lipophilic chains on the acidic and basic components against gave inadequate ionic salt formation, these structural differences responsible for sensitivity to mechanical strain. The mechanical strength of liquid paraffin gels decreases with increasing total carbon number in the acidic and basic parts of gelator chains (Table 2).

The more lasting elastic property indicator is the increase in the stress of the crossing-over point. The crossing-over point gave the same results as the storage module. When the stress increased, the elasticity of the gel was so lasting (Table 2). The increase of the chain proportion from 12 to 16 carbons in the acidic part decreased the gel elasticity, producing an inconsistent gelator structure for the gel but increasing its Npx loading capacity. The B_1A_3/**LP and** B_2A_3/**LP** gels systems showed the most excellent interaction and the most suitable **HLB** (hydrophile–lipophile-balance) values to form the most elastic gel in **LP**. The loss factors of loaded forms decreased ($tan\delta = G''/G'$) in **LP** indicating the organogel strength and their order were found to be dependent on the chain length in the acidic parts ($B_1A_3 < B_1A_4 < B_1A_5$) ($B_2A_5 < B_2A_3$) in the gelator structures, respectively. It is shown that lipophilic balance is essential for the gelator framework (Table 2).

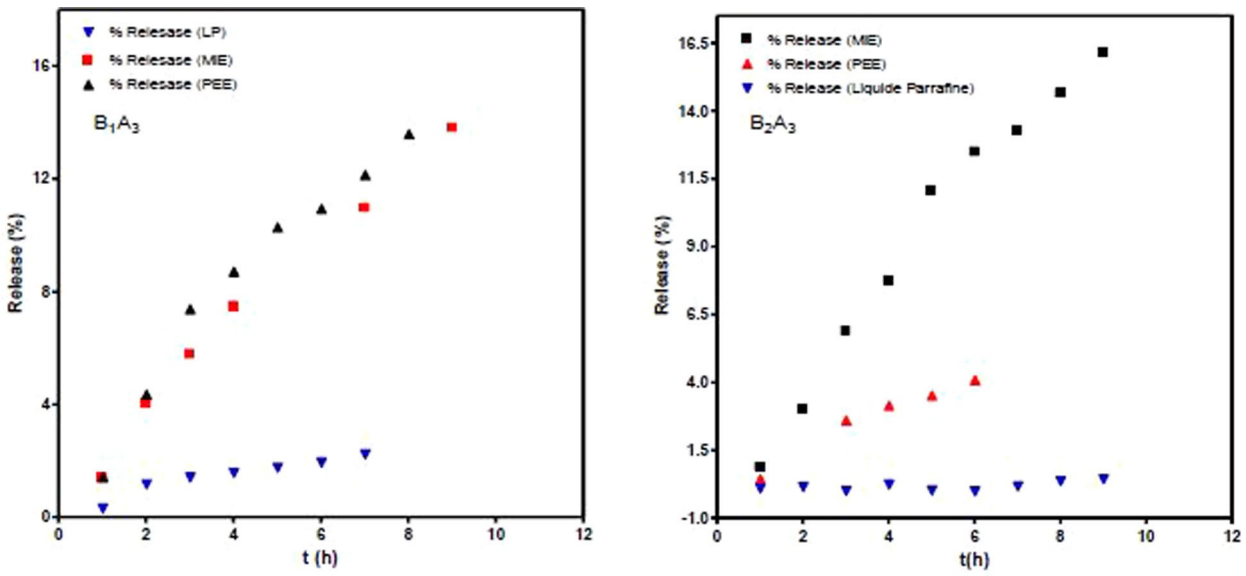

Figure 11. The time-dependent cumulative release rate from Npx (1.5 mg) loaded $\mathbf{B_1A_3}$ (5 mg) and $\mathbf{B_2A_3}$ (4 mg) gels in 1 mL of different solvents at pH 7.4 (0.1 M phosphate buffer) and 25 °C. Each point represents mean ± S.D. ($n = 3$)

Higher G′ values about G″ were observed in most formulations in LP even after Npx was included. G′ values were 3–19 times higher than those observed for G′, resulting in viscoelastic behaviour for the different formulations. It can be argued that Npx interacts with the supramolecular structure of B_mA_n-type organogels with different modalities depending on the total number of carbons in their alkyl chains and the type of gelling fluids.

G′ describes the elasticity of a material. Higher G′ values relative to G′′ values correspond to the more crucial structural organization within a system. Figure 9 shows the storage modules (G′) of multiple gel systems as a function of frequency for 24 hours and 50 days after gels preparation with different storage times. In these two different cases, the loss modulus (G″) was lower than the storage modulus (G′). Rheological analysis results for Npx loaded B_1A_3/MIE for 50 days of storage showed higher G′ > G″ than 1-day storage modulus. Also, higher viscose modulus and complex viscosity between final and 50-day rheological profiles were observed here, emphasizing the structural stability of the formulations. This phenomenon could be due to several reasons.

The systems may cross-link, or some components in the gels may volatilize, which is more likely for organogels, leading to increased elasticity.[29] This feature is essential for topical treatment, which indicates whether the formulation allows some deformation without loss of gel structure and stability. When the time-dependent G′ and G″ curves are shown as double logarithmic charts, only a slight slope indicating that elastic behaviour dominates viscous behaviour appears as parallel straight lines throughout the entire frequency range Figure 10.

In this study, the relationship between drug release and the rheological and mechanical properties of $\mathbf{B_mA_n}$ gels, which have a significant effect on drug release, as observed in topical gel systems, was investigated. Studies have shown that gel viscosity decreases with increasing Npx concentration. To significantly improve topical therapy, the residence time of drugs on the skin should be increased. Furthermore, applying a thinner layer of semi-solid to the skin requires a lower viscosity, resulting in faster absorption of the drug.[5,30] The end value of the linear viscoelastic region indicates that the steady-state structure was disturbed or even destroyed (Figures 6 and 8). The Npx-loaded **B_2A_3/MIE** and the **B_1A_3/PEE** matrix were broken down at small stress values applying moderate strain, but **B_2A_3/PEE** showed an extended linear region. We can explain the different stress sweep behaviours with the fluid differences. The short linear part of the **B_2A_3/MIE** and the **B_1A_3/PEE** indicates that these structures are fragile. The crystalline gel nature of the **B_2A_3/MIE** and the **B_1A_3/PEE** networks are responsible for mechanical strain sensitivity. Npx-loaded B_2A_3/PEE has a more extended linear region. The reason why it seems more resistant to mechanical strain is the highly intermeshed structures (Figure 6). In addition, the minimum loss tangent (tan δ) values in the linear viscoelastic region show that the elastic properties are more dominant than the viscous ones (Table 1). Among $\mathbf{B_mA_n}$ gels, the formulation containing $\mathbf{B_2A_3}$ myristoyl lysine as base component and isopropyl palmitate(**PIE**) as oil had the lowest loss tangent (tan δ) values and the most significant storage modulus (G′) value (Table 1). Easy spreadability means low yield value in application. In inflammatory and sensitive skin applications, this feature is significant for a dermal product. It is seen that the endpoints of the linear viscoelastic field are correlated with the yield points in the oscillation stress sweep test. In the crossing-over point values, it is seen that elastic properties dominate up to high-stress values at the expense of viscous properties (Tables 1 and 2). Broad linear viscoelastic regions and great crossing-over point values are seen, signs of

the structure's ability to resist external stresses to a greater extent.

Fourier transform infrared spectroscopy

Any deviation from normal FTIR spectra, such as the appearance (or disappearance) of a peak corresponding to a specific functional group, was employed to provide information about the possibility of interaction. Primary peaks of Npx alone were observed at 3245, 3181, 3085, 1726, 1683, 1602, 1456, 1391,1266,1226, 1159, 1025,817, and 670 $cm^{-}1$, confirming the purity of the drug sample according to established standards. Major peaks of B2 A3/LP gel' were observed 3335, 3286, 1644, 1537, 1508. Above diagnostic peaks which is belong to Npx and B2 A3 gelator were screened from the B2 A3/LP/Npx formulation at 1744, 1729, 1706, 1683, 1652, 1606, 1558, 1536, 1461, and 1377, 1265, 1228, 1175 cm. Although the major peaks of Npx in the formulation obscured due to a large volume of entrapped LP fluid. The primary Npx peaks were observed even when the drug was combined with an excipient. In the B2 A3/LP-Npx formulation, the IR spectra of the drug with excipients showed most of the above-mentioned characteristic peaks with insignificant shift and reduced intensity. This confirmed the absence of any drug-excipient interaction in the B2 A3/LP-Npx formulation.

Release studies

Among $\mathbf{B_mA_n}$ formulated two-component gelators (N^{ε}-Alkanoyl-*L*-lysine ethyl ester- *N*-alkanoyl-*L*-amino acid derivatives) $\mathbf{B_1A_3}$, $\mathbf{B_2A_3}$, which have phenylalanine amino acid as a part of the acidic component, all of them demonstrated good gelation ability in LP, PEE and MIE than $\mathbf{B_1A_1}$, $\mathbf{B_1A_2}$ gelators including alanine and leucine amino acids in the acid component, respectively. For this reason, phenylalanine included amino acid parts in acidic components, designated as $\mathbf{B_1A_3}$, and $\mathbf{B_2A_3}$, that formed the most stable gel in pharmaceutic fluids and were tested in a drug release study.

Solvent effect on the drug release

It is seen in Figure 11. The percentage of cumulative drug release rate % from ($\mathbf{B_1A_3}$) **and** ($\mathbf{B_2A_3}$) gels in **PEE**, **MIE** and LP were found 17%, 12.5%, 1.5% and 16.5%, 7.5%, 1.1%, respectively at the end of 24 hours.

In conclusion, the release rate for both gelators was very low when liquid paraffin was used as the gelling fluid. However, the release rate for both gelators was faster when **MIE** and **PEE** were used as gelling fluids. The natures of both the gel matrix and the active drug may influence the *in vitro* drug release, especially the viscosity of the matrix, the drug solubility, the partition of drug molecules in the matrix, and the interaction between the drug molecules and other ingredients of the gel. Compared Npx loaded $\mathbf{B_1A_3}$/**LP** with $\mathbf{B_1A_3}$ in **MIE** and **PEE** fluids showed a slower release rate due to higher mechanical strength and viscosity due to the very high stability of the $\mathbf{B_1A_3}$ in **LP** (G'/G'' ratio is 19.1).

The effect of pH on the release of the drug

The result showed that the drug release increased at pH 7.0 and 7.4 depending on the solubility of Npx. At lower pH (5.5) due to the low solubility of Npx, the drug release was found slow. In conclusion, this result showed that drug release could be controlled by pH (Figure 12).

Effect of Drug Concentration

It is seen from (Figure 13), at low drug concentrations, the release rate was not changed a lot. However, when the drug concentration was increased to 3 mg, the release rate was increased immediately. Therefore, one of the most critical parameters in terms of cumulative drug release percentage is drug concentration. The study showed that the complex viscosity decreases when the drug concentration increases and is directly proportional to the drug concentration.

As a result, when the Npx concentration increases, the complex viscosity of the gel formulations decreases, and the spreadability decreases due to the increase in the resistance between the layers. In contrast, with the addition of Npx to the gelator/liquid system, the G′ and complex viscosity η* values, which indicate an increase in the G′/G″ ratios, decreased (Table 1). This effect is due to the interference introduced by the Npx molecules in the three-dimensional structure formation of the gel and provides the occurrence of a superior organization.[30] Npx addition to the gel evoked structural

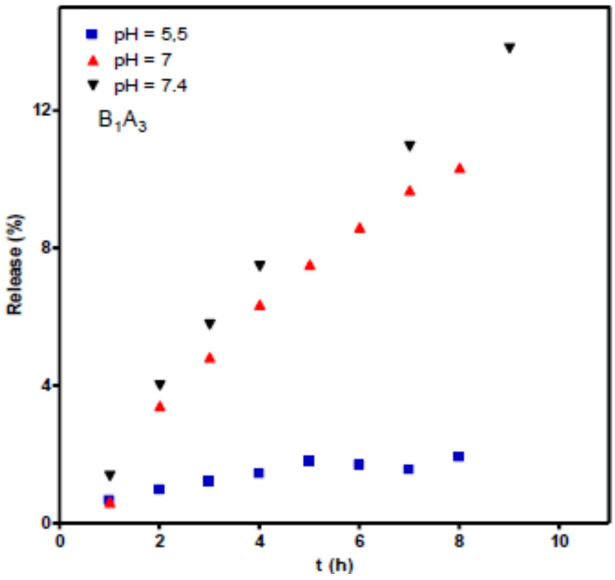

Figure 12. The effect of pH on the time-dependent release of Npx (1.5 mg) from ($\mathbf{B_1A_3}$) gel prepared in MIE at different pH (0.1 M phosphate buffer) and 25 °C. Each point represents mean ± S.D. ($n = 3$)

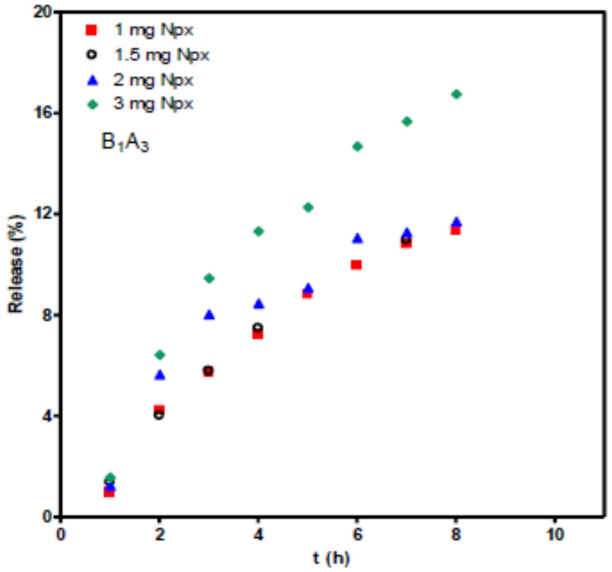

Figure 13. The time-dependent release rate of Npx from B_1A_3 gel at different drug concentrations in **MIE** at pH 7.4 (0.1 M phosphate buffer) and 25 °C Each point represents mean ± S.D. ($n = 3$)

changes and was determined using rheology. B_1A_3 in MIE showed a decreased elastic modulus with increased Npx concentration (Figure 14).

When the loaded drug concentration was high, the release rate was faster due to the rapid degradation of the gel structure. At low drug concentrations, the release rate was closer to each other. In the case of high drug concentration, the release rate was increased. The column chart shows that the release rate was raised as the proportion of loaded drugs increased (Figure 15). This result indicated that the Npx release rate could be controlled together with the adjustable drug dose.

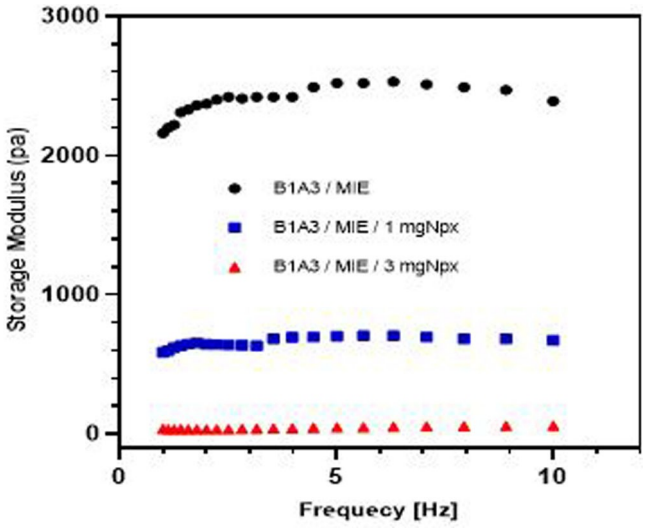

Figure 14. The elasticity modulus of B_1A_3/**MIE** gel samples depending on the Npx concentration. The G′ was measured at two different Npx concentrations at 25 °C. Gelator concentration: 7 mgmL^{-1} Each curve presents the mean value of three tests.

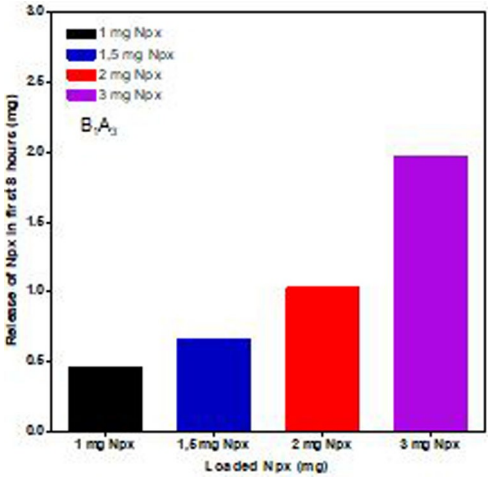

Figure 15. The released quantity of Npx (mg) in the first 8 hours vs. different loaded drug doses (mg) at pH 7.4. Gel matrix: (B_1A_3) gelator (5 mg) in 1 mL **MIE**

Drug Release Kinetics

Correlation coefficient (R^2) of 10-h drug release profile (Figure 16) was ~0.99, which indicated that the model fitted the release behavior of organogel system well. The highly linear responses (r~0.99) of the accumulated release amounts versus the square root of time indicated that the release of Npx from these gels closely followed the Higuchi equation and matrix diffusion kinetics. The Higuchi equation (The equation 4) was used to measure drug release from organogels into the artificial physiological fluid. This equation both facilitates device optimization and enables us to understand the underlying drug release mechanisms better.[31]

$$M_t/M_\infty = kt^{1/2} \quad \text{(Eq. 4).}$$

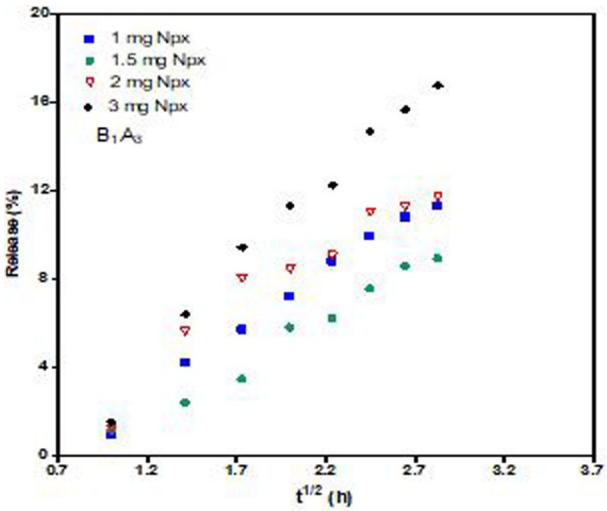

Figure 16. The time-dependent release rate of Npx (%) vs. square root of time ($t^{1/2}$). (B_1A_3) gelator (5 mg) in (1 mL) **MIE** at pH 7.4 at different drug concentrations. Each curve presents the mean value of three tests.

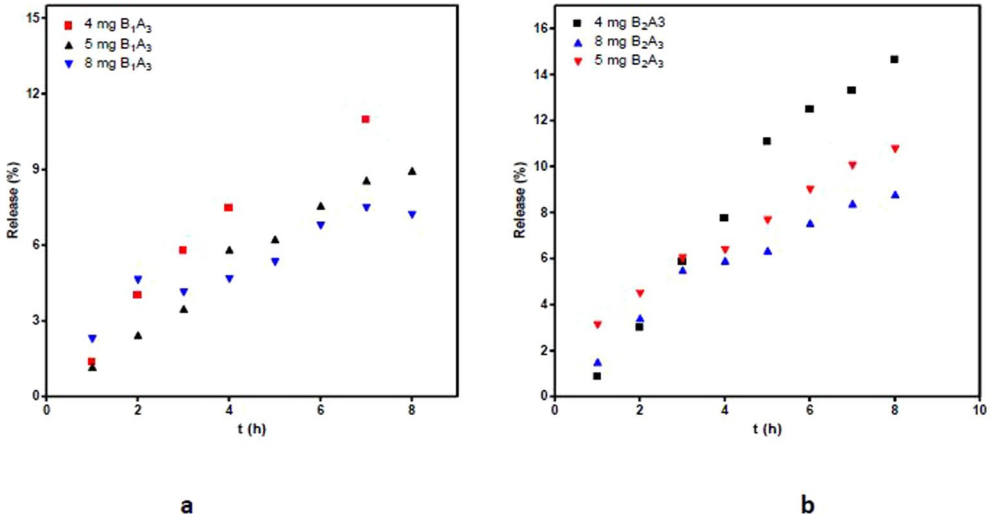

Figure 17. The release (%) vs time (t) graph of Naproxen (1.5 mg) with different gelators; **a)** (**B_1A_3**) and **b)** **B_2A_3** concentrations in **MIE** at pH 7.4. Each curve presents the mean value of three tests.

M_t is the absolute cumulative amount of drug released at time t, M_∞ is the absolute cumulative amount of drug released at infinite time, k is a constant reflecting the design variables of the system, and t is the time. The linear responses of the cumulative release amounts versus the square root of time showed that Npx release from the gels followed the Higuchi equation and matrix diffusion kinetics with confidence (r ~0.99).[32,33] Examples of the fitness of data to the Higuchi equation are shown in Figure 16, Table 3) They all follow the Higuchi equation (Eq. 3) with reasonable confidence.

Effect of Gelator Concentration on the Drug Release

It is seen that from the graph, drug release was decreased when the concentration of the gelator was increased (Figure 17). The decrease in drug release is because the percentage of drug release % (as a diffusional route) depends on the fiber's entanglement in the solid structure network formed by gelator molecules. Gelator aggregation or fibers are responsible for the three-dimensional structural network that is immobilized in the liquid phase. As a result, it prevented passing the drug outside the matrix by cross-linking.

In conclusion, it is caused to decreasing drug release. Increasing (**B_1A_3**) concentration in **MIE f**rom 0.46% to 0.92%, the initial release rate considerably reduced, from 18.75% to 7.21%, respectively; that is release rate shows a 2.6-fold decrease. Similarly concentration of (B_2A_3) gelator in MIE increases; in this case, the initial release rate reveals a 1.37-fold decrease, slightly reduced, from 14.75% to 10.76%, respectively. This result showed that the gelator concentration could control drug release.

One of the parameters used to measure viscosity, spreadability, and cumulative drug release percentage is gelator concentration. In this study, it has been shown that when the gelator concentration increases, the viscosity also increases, and it is directly proportional to the gelator concentration. Therefore, the increase in the (**B_1A_3**) concentration increases the gel formulations' viscosity, leading to increased resistance between the layers and reducing the spreadability. Thus, the cumulative percent of drug release decreased as the viscosity of the formulations increased, and these results were consistent with previous study findings.[34] As a result, a more substantial structure can be obtained when using higher concentrations of gelling agents observed in semi-rigid and semi-flexible structures.

Conclusions

We demonstrated that *N*$^{\varepsilon}$-alkanoyl-*L*-lysine ethyl ester/*N*-alkanoyl-*L*-phenylalaninates gelling agents had been constructed two-component gelling strategy, applied as a drug carrier in friendly solvents, commonly used in the cosmetics industry. A novel organogelator based on lysine and phenylalanine amino acids is tailed by an alkanoyl chain, and then their salt forms have occurred as a two-component system. The formation of three-dimensional multi-porous networks with acid-base interactions and strong hydrogen bonds between amino acids is considered a driving force in forming stable organogels.

These systems may prove to have the edge in contrast to the other lipid-based system, such as cheap raw materials, ease of loading, simple dose adjustability, skin spreadability, and improved drug retention times. These organogelators gain an advantage over the other delivery technique, especially in topical application. The rheology parameters can be used to estimate structure strength, which is the G′, G″ values and the low slope G″/G′ ratio corresponding to a strong structure. As a result, it was observed that there was a relationship between rheological properties and release profiles. Moreover, liquid paraffin, PEE, and **MIE** were chosen as gelation fluids owing to being natural and biodegradable and employed in the

pharmaceutical industry. The entrapment of Npx within the combination (B_1A_3)/**MIE** gel matrix has been achieved with the high drug/gelator ratio of 100% (w/w) without gel disruption.

The in vitro drug release showed that **B1 A3** and **B2 A3** gelators in **MIE** and **PEE** fluids exhibited the highest release rate, while the extended-release rate was procured with both the same gelators in LP.. We believe that creating these new materials described for developing novel drug delivery devices applied in this work shows promising properties with diverse and tunable properties, tailored to tunability and controllable features

The *in vitro* drug release results showed that B_1A_3/**PEE** exhibited the highest drug release rate among the gels studied, and the percentage release was 17% at the first 10 h; in contrast, B_1A_3/**LP** exhibited the lowest drug release rates the percentage release was 1.5% at the first 10 h. Thus, the active drug and other gels' ingredients and interactions will affect the drug release profiles from different gels.

Acknowledgements

The authors thank The Scientific and Technological Research Council of Turkey (TUBITAK) for financially supporting this research (Project No. 113Z142). And also we are grateful to The University of Dicle research council (DÜBAP) for financial support of this work. And also we are greatful to The University of Dicle University Science And Technology Application And Research Center (DUBTAM).

Conflict of Interests

The authors declare that they have no conflict of interest.

Data Availability Statement

The data that support the findings of this study are available from the corresponding author upon reasonable request.

Keywords: Controlled drug release · low molecular weight organogelators (LMWOGs) · Rheology · Small molecule gelling agent (SMGA) · Supramolecular gels

[1] Y. Ohsedo, *Gels.* **2016**, *2*, 2–11.
[2] L. Zeng, X. Lin, P. Li, F. Liu, H. Guo, W. Li, *Prog. Org. Coat.* **2021**, *159*, 106417.
[3] M. A. Kuzina, D. D. Kartsev, A. V. Stratonovich, P. A. Levkin, *Adv. Funct. Mater.* **2023**, *33*, 2301421.
[4] G. Vanitha, D. Subhashis, B. P. Hima, B. M. Niranjan, *Indian J. Res. Pharm. Biotechnol.* **2014**, *2*, 976–981.
[5] L. E. Cloé, K. Plamen, V. Gaëlle Roullin, *J. Controlled Release* **2018**, *27*, 11–20.
[6] J. Brus, W. Albrecht, F. Lehmann, J. Geier, J. Czernek, M. Urbanova, L. Kobera, A. Jegorov, *Mol. Pharmaceutics* **2017**, *14*, 2070–2078.
[7] N. Aktas, D. Alpaslan, E. T. Dudu, *Front. Mater.* **2022**, *9*, 1–10.
[8] I. Sadeghi, J. Byrne, R. Shakur, R. Langer, *J. Controlled Release.* **2021**, *331*, 503–514.
[9] R. Langer, *Science.* **2001**, *293*, 58–59.
[10] M. C. Branco, D. J. Pochan, N. J. Wagner, J. P. Chneider, *Biomaterials.* **2009**, *30*, 1339–1347.
[11] F. F. Hamad, *IJPSR.* **2019**, *10*, 3487–3507.
[12] S. Avramiotis, V. Papadimitriou, E. Hatzara, V. Bekiari, P. Lianos, A. Xenakis, *Langmuir.* **2007**, *23*, 4438–4447.
[13] H. J. Smith, H. J. Williams, Introduction to the Principles of Drug Design and Action, 4th Ed, *Taylor and Francis Group*, USA, **2018**, 216–230.
[14] A. Mayr, G. Klambauer, T. Unterthiner, M. Steijaert, J. K. Wegner, H. Ceulemans, D. A. Clevert, S. Hochreiter, *Chem. Sci.* **2018**, *9*, 5441–5451.
[15] D. T. Makhıja, R. R. Somanı, A. V. Chavan, *Indian J. Pharm. Sci.* **2013**, *75*, 353–357.
[16] S. Uzan, D. Barıs, M Çolak, H. Aydın, H. Hoşgören, *Tetrahedron.* **2016**, *72*, 7517–7525.
[17] M. V. Torre, J. Forcada, The Potential of Stimuli-Responsive Nanogels in Drug and Active Molecule Delivery for Targeted Therapy. *Gels.* **2017**, *3*, 1–37.
[18] M. Colak, D. Barış, M. Evcil, N. Demirel, H. Hoşgören, *Soft Mater.* **2018**, *16*, 289–302.
[19] N. Schork, S. Schuhmann, O. Gruschke, D. Groß, K. Zick, H. Nirschl, G. Guthausen, Chapter Five – Recent MRI and diffusion studies of food structures, Annual Reports on NMR Spectroscopy, Academic Press, London, **2020**, *100*, 203–264.
[20] V. Sanna, A. Mariani, G. Caria, M. Sechi, *Chem. Pharm. Bull.* **2009**, *57*, 680–684.
[21] M. Gasperlin, J. Kristl, J. Smid-Korbar, *S. T. P. Pharma Sci.* **1997**, *7*, 158–163.
[22] M. Korhonen, H. Niskanen, J. Kiesvaara, J. Yliruusi, *Int. J. Pharm.* **2000**, *197*, 143–151.
[23] I. Rosalina, M. Bhattacharya, *Carbohydr. Polym.* **2002**, *48*, 191–202.
[24] S. Cao, X. Fu, N. Wang, H. Wang, Y. Yang, *Int. J. Pharm.* **2008**, *357*, 95–99.
[25] L. Zhen, C. Jinxu, L. Heran, L. Hongzhuo, H. Fei, L. Zhenyun, T. Chao, L. Sanming, *Drug Delivery* **2016**, *23*, 3168–3178.
[26] M. A. Kuzina, D. D. Kartsev, V. S. Alexander, A. L. Pavel, *Adv. Funct. Mater.* **2023**, *33*, 2301421.
[27] G. Sharma, N. Devi, K. Thakur, A. Jain, O. P. Katare, *Drug Delivery Transl. Res.* **2018**, *8*, 398–413.
[28] D. Vasiljevic, G. Vuleta, M. Primorac, *Int. J. Cosmet. Sci.* **2005**, *27*, 81–87.
[29] R. Brummer, *Rheology essentials of cosmetic and food emulsions*, Berlin: Springer, **2006**, 180.
[30] F. M. Mady, H. Essa, T. Tarek El-Ammawi, H. Abdelkader, A. K. Hussein, *Drug Des. Dev. Ther.* **2016**, *10*, 1101–1110.
[31] T. Higuchi, *J. Pharm. Sci.* **1963**, *52*, 1145–1149.
[32] P. Kirilov, S. Rum, E. Gilbert, *Int. J. Cosmet. Sci.* **2014**, *36*, 336–346.
[33] A. R. Patel, M. Babaahmadi, A. Lesaffer, K. Dewettinck, *J. Agric. Food Chem.* **2015**, *63*, 4862–4869.
[34] M. Pandey, V. Belgamwar, S. Gattani, *Drug Delivery* **2010**, *17*, 38–47.

Manuscript received: July 28, 2023